



## MECHANISTIC INTEGRATION OF THERMODYNAMIC QUALITY DURING TRANSIENT AIR BLAST FREEZING OF EXPORT-GRADE SHRIMP

Faizin Adi Nugroho<sup>1\*</sup>, Yaser Krisnafi<sup>1</sup>, Liya Tri Khikmawati<sup>1</sup>,  
RR. Rادیpta Lailatussifa<sup>2</sup>, Ika Astiana<sup>3</sup>, Citra Zaskia Pratiwi<sup>1</sup>

<sup>1</sup>Fisheries Mechanization Dept., Sidoarjo Marine and Fisheries Polytechnic  
Buncitan st., Sedati, Sidoarjo, East Java, Indonesia, 61253

<sup>2</sup>Fishery Product Processing Dept., Sidoarjo Marine and Fisheries Polytechnic  
Buncitan st., Sedati, Sidoarjo, East Java, Indonesia, 61253

<sup>3</sup>Marine Product Processing Dept., Jembrana Marine and Fisheries Polytechnic  
Pengembangan st., Negara, Jembrana, Bali, Indonesia, 82218

Submitted: 21 November 2025/Accepted: 13 March 2026

\*Correspondence: [faizin.adi89@gmail.com](mailto:faizin.adi89@gmail.com)

**How to cite (APA Style 7<sup>th</sup>):** Nugroho, F. A., Krisnafi, Y., Khikmawati, L. T., Lailatussifa, R. R. R., Astiana, I., & Pratiwi, C. Z. (2026). Mechanistic integration of thermodynamic quality during transient air blast freezing of export-grade shrimp. *Jurnal Pengolahan Hasil Perikanan Indonesia*, 29(6), 562-581. <http://dx.doi.org/10.17844/65efk717>

### Abstract

Shrimp quality is highly sensitive to freezing stability during early post-harvest handling. Although air blast freezers (ABF) are widely applied in industrial processing, the quantitative linkage between transient thermodynamic degradation and early microstructural deterioration remains insufficiently resolved. This study aims to investigate the mechanistic relationship between early-stage ABF performance decay and time-resolved shrimp quality changes during the first 6 h of freezing. An integrated experimental approach was conducted by combining in-situ measurements of airflow velocity, air-side temperature differential ( $\Delta T$ ), evaporator frosting mass, cooling capacity (Q), and actual coefficient of performance (COP) with laboratory analyses of ice crystal size, water-holding capacity (WHC), drip loss, texture, pH, melanosis, and TVB-N. The results demonstrate a progressive frosting accumulation (0.09-1.50 kg) that reduced airflow (4.38-2.62 m s<sup>-1</sup>), suppressed cooling capacity (28.99-20.98 kW), and deteriorated COP (3.51-2.33). Frosting mass explained up to 97-98% of COP and Q variance. Sequential regression analysis confirmed a strong mechanistic pathway: COP decline significantly enlarged ice crystals ( $R^2 = 0.97$ ), which reduced WHC ( $R^2 = 0.96$ ) and increased drip loss ( $R^2 = 0.98$ ). These findings indicate that transient thermodynamic instability, rather than steady-state temperature compliance alone, governs early structural degradation. The study repositions COP as a predictive upstream control parameter linking machine performance to product integrity and provides a performance-oriented framework for HACCP-integrated monitoring and early operational optimization in industrial shrimp freezing systems.

Keywords: COP, frost effect, freezing temperature fluctuations, shrimp quality

### Integrasi Mekanistik Termodinamika-Kualitas selama Air Blast Freezing Transien pada Udang Kelas Ekspor

#### Abstrak

Mutu udang sangat dipengaruhi oleh stabilitas proses pembekuan pada tahap awal pascapanen. Meskipun *air blast freezer* (ABF) banyak diterapkan dalam pengolahan industri,

hubungan kuantitatif antara degradasi termodinamika transien dan kerusakan mikrostruktur awal belum menjelaskan secara komprehensif. Penelitian ini bertujuan mengkaji hubungan mekanistik antara penurunan performa awal ABF dan perubahan mutu udang secara time-resolved selama 6 jam pertama pembekuan. Pendekatan eksperimental terintegrasi dilakukan melalui pengukuran in-situ kecepatan aliran udara, perbedaan suhu udara masuk-keluar ( $\Delta T$ ), akumulasi frosting evaporator, kapasitas pendinginan ( $Q$ ), dan koefisien performa aktual (COP), yang dikombinasikan dengan analisis laboratorium terhadap ukuran kristal es, water-holding capacity (WHC), drip loss, tekstur, pH, melanosis, dan TVB-N. Hasil menunjukkan peningkatan frosting (0,09-1,50 kg) yang menurunkan airflow (4,38-2,62 m s<sup>-1</sup>), kapasitas pendinginan (28,99-20,98 kW), dan COP (3,51-2,33). Akumulasi frosting menjelaskan hingga 97-98% variasi COP dan  $Q$ . Analisis regresi berurutan mengonfirmasi jalur mekanistik yang kuat: penurunan COP memperbesar kristal es ( $R^2 = 0,97$ ), yang selanjutnya menurunkan WHC ( $R^2 = 0,96$ ) dan meningkatkan drip loss ( $R^2 = 0,98$ ). Temuan ini menunjukkan bahwa ketidakstabilan termodinamika bersifat transien (sementara dan berfluktuasi), bukan sekadar kepatuhan terhadap suhu steady-state (suhu stabil rata-rata) saja, yang sebenarnya justru mengendalikan degradasi struktural awal. Penelitian ini memosisikan COP sebagai parameter kontrol prediktif yang menghubungkan performa mesin dengan integritas produk serta memberikan dasar optimasi berbasis kinerja dan monitoring terintegrasi HACCP pada sistem pembekuan udang skala industri.

Kata kunci: COP, efek bunga es, fluktuasi suhu beku, kualitas udang

## INTRODUCTION

Shrimp is a high-value fishery commodity with a continuously increasing market demand. Temperature instability during air blast freezer (ABF) operation constitutes not only a thermodynamic inefficiency but also a direct economic risk factor in shrimp export systems (Prambudia & Sriwana, 2025). Transient temperature fluctuations accelerate microstructural damage, increase drip loss, downgrade product grading, and elevate the probability of buyer rejection, thereby reducing market prices and contractual reliability (Anggrahini *et al.*, 2015; Lin *et al.*, 2022). Consequently, inadequate thermal control in ABF processing translates into measurable financial losses for exporters through value depreciation, return penalties, and diminished global competitiveness (Samanta & Imroatin, 2025). The post-harvest storage conditions and freshness of shrimp significantly determine their overall quality. Enzymatic activity, microbiological processes, and lipid oxidation can rapidly deteriorate shrimp quality, resulting in noticeable changes in color, texture, and flavor (Cheng *et al.*, 2025).

Consequently, to maintain shrimp quality throughout distribution and storage, the implementation of an efficient preservation

method is essential (Liu *et al.*, 2024; Zhao *et al.*, 2024; Zhu *et al.*, 2024). Although previous studies have extensively examined shrimp freezing quality, ice crystal formation, drip loss, and energy efficiency in air blast freezer systems, the direct link between transient ABF performance degradation and early stage microstructural quality loss remains unclear. The novelty of this study lies in the integration of frost-induced thermodynamic decay, represented by airflow reduction, temperature differential changes, and COP decline, with shrimp quality kinetics, including ice crystal enlargement, water-holding capacity reduction, drip loss, and texture degradation. Therefore, this study aimed to establish a predictive thermodynamic framework that positions COP as an upstream control parameter for maintaining structural integrity and quality consistency in export-grade frozen shrimp.

Previous studies have discussed the application of freezing technology in the fisheries industry. Research conducted by Klunklin *et al.* (2025) focused on shrimp products and revealed that rapid freezing using an air blast freezer preserved shrimp quality more effectively than slow freezing methods. In addition, Duan *et al.* (2025) and Zhao *et al.* (2024) demonstrated that both



freezing rate and temperature significantly influence the quality of fishery products during storage. The application of various freezing technologies for shrimp commodities demonstrates that equipment performance plays a crucial role in preserving the structural, functional, and sensory integrity of products throughout the cold-chain storage period. Hermes *et al.* (2021) highlighted that rapid-freezing methods, such as air blast freezers (ABF), generate smaller and more uniformly distributed ice crystals, thereby minimizing tissue damage, reducing moisture loss, and mitigating protein degradation commonly observed in slow-freezing processes (Sun *et al.*, 2023a).

Conversely, conventional freezing at temperatures above  $-20^{\circ}\text{C}$  increases drip loss, accelerates myofibrillar denaturation, and decreases water-holding capacity during thawing and subsequent heat treatment (Wei *et al.*, 2024). In this context, case-based comparisons reveal that freezer performance, characterized by freezing rate, temperature stability, and airflow management, correlates directly with the final quality attributes of shrimp, including texture, color, and nutritional retention (Tan *et al.*, 2021; Jin *et al.*, 2018). Overall, evidence from the literature underscores that optimizing freezing technology is not merely a technical consideration but a key determinant of the success and reliability of export-grade frozen shrimp supply chains.

Despite the extensive industrial reliance on air blast freezers (ABF) for shrimp freezing, existing studies predominantly assess end-product freshness indicators (pH, TVB-N, and microbial load) without explicitly resolving how real-time ABF operational behavior governs microstructural quality deterioration. Current literature typically evaluates air temperature, freezing time, or airflow as isolated variables, while evaporator frosting, airflow instability, and thermal non-uniformity, although frequently acknowledged, are rarely quantified and analyzed as an integrated thermodynamic system. Furthermore, prior investigations have demonstrated that temperature

fluctuations and slow freezing rates exacerbate ice recrystallization and protein denaturation.

However, the direct coupling between machine efficiency metrics (COP, cooling capacity, and  $\Delta T$ ) and physical quality indicators, such as ice crystal size, WHC, and texture loss, remains largely unexplored. In particular, no study has systematically linked the declining COP and evaporator frosting dynamics to the early stage freezing window that governs irreversible muscle damage. Additionally, HACCP-based controls in frozen seafood operations are often implemented as procedural compliance tools rather than being validated against real thermodynamic and airflow data. This creates a critical knowledge gap in which microstructural degradation can occur under microbiologically safe conditions but remains undetected by conventional quality monitoring frameworks.

To address this deficiency, the present study evaluated the ABF holistically by assessing the cooling capacity, machine efficiency, freezing time, inlet-outlet temperature profiles, frosting effects, and airflow velocity (Alar *et al.*, 2024), while contextualizing these parameters against the known mechanisms of muscle structural deterioration. This study presents a comprehensive and experimentally validated framework that integrates ABF mechanical performance with evaporator frosting behavior and time-resolved shrimp quality responses. Unlike prior studies that assess equipment and products separately, this study establishes a direct causal linkage between operational deviations within the ABF system and the physical quality deterioration of shrimp muscle, thereby redefining ABF evaluation from a machine-centered to a process product coupled perspective.

## MATERIALS AND METHODS

The design and structural parameters of the air blast freezer being studied are located in the modern processing teaching factory (TEFA), which is currently rented by PT. XYZ for freezing fishery products and processed foods from frozen fishery products before export, with the technical specifications listed in Table 1.

Table 1 Bitzer S6F-30.2Y-40P ABF technical specifications

Parameters	Value
Compressor type	Semi hermetic, 2 stage piston
Number of cylinders	6 cylinder
Serial number (S/N)	1600810283
Displacement (1450 RPM)	101.1 m3/h (LP), 50.5 m3/h (HP)
Motor power	30 HP/ 22 KW
Operating voltage	380 - 420 V (50 Hz) / 440 - 480 V (60Hz), 3 phase
Maximum current	53 A
Maximum power	30.1 KW
Initial current (LRA)	135/220 A (Y/YY)
Oil capacity	4.75 liters (BSE2 for R404A/R507A)
Net weight	234 Kg
Suction line connection	42 mm ( 1 5/8" )
Discharge line connection	35 mm ( 1 3/8" )
Maximum pressure	28 bar
Supported refrigerants	R404A, R507A, R448A, R449A, R22 (oil based B5.2)

The (ABF) system used in this study was designed based on BITZER refrigeration components to ensure stable low-temperature operation during shrimp freezing. Table 2 presents the main design specifications of the

ABF unit, including its refrigeration capacity, operating conditions, and supporting components used as the basis for the performance evaluation.

Table 2 BITZER brand air blast freezer (ABF) design specifications

No.	Data	Capacity	
1.	Dimensions	Length	3.5 m
		Width	2.5 m
		Height	2.5 m
2.	Air blast freezer capacity	2 ton	
3.	Polyurethane walls	Thick	150 mm
		Room	-35°C
4.	Temperature	Environment	30°C
		Evaporation	-30°C
		Floor	10°C
5.	Air humidity	Room	25%
		Environment	20%
6.	2 Fan	800 W	
7.	Heater defrost	Coil	5.600 W
		Dry tray	5.600 W



The physical properties of the shrimp products were characterized to provide baseline information on product dimensions, mass, and thermal-related attributes relevant to the freezing performance analysis, as summarized in Table 3.

**ABF Test Method**

Field measurements were conducted using both mechanical and digital instruments in the air-blast freezer system. The collected data included temperature and pressure variables measured at several critical points within the system at specific time intervals throughout the operational periods (Hermes *et al.*, 2021). Temperature monitoring was conducted using RTD PT100 sensors (Class A, ±0.15°C accuracy) with stainless steel probes (Omron E52 Series). The air velocity inside the freezing chamber was measured using a Krisbow digital anemometer (±3% accuracy, 0.01 m/s resolution) to quantify the airflow variations associated with the development of frosting and heat transfer performance. All measurements were recorded at fixed time intervals to capture the transient thermodynamic behavior during the early freezing stage. The primary objective of this measurement was to observe the system performance, identify the patterns of temperature and pressure fluctuations, and evaluate the overall system efficiency (Badri *et al.*, 2021). The analysis and evaluation included:

1. Calculate the ABF air flow rate

$$Q_{air} = A \times V$$

Q = air flow rate capacity m<sup>3</sup>/s

A = cross-sectional area of air duct m<sup>2</sup>

V = air flow rate m/s

2. Efficiency of temperature distribution in ABF

$$\Delta t = T_{inlet} - T_{outlet}$$

T<sub>inlet</sub> = air temperature entering the ABF room °C

T<sub>outlet</sub> = outlet air temperature to the ABF room °C

3. Cooling capacity

$$Q_1 = m \times C_p \times \Delta t$$

$$Q_2 = m \times L_f$$

Q = cooling capacity (kJ or kW)

m = frozen shrimp mass (Kg)

C<sub>p</sub> = specific heat capacity of shrimp before freezing (kJ/Kg)

Δt = initial shrimp temperature – shrimp temperature reaches freezing point (°C)

L<sub>f</sub> = latent heat of freezing shrimp (kJ/Kg)

4. Frosting effect on the evaporator

$$Q_1 = m \times C_p \times \Delta t$$

$$Q_2 = m \times L_f$$

Q = cooling capacity (kJ or kW)

m = frozen shrimp mass (Kg)

C<sub>p</sub> = specific heat capacity of shrimp before freezing (kJ/Kg)

Δt = initial shrimp temperature – shrimp temperature reaches freezing point (°C)

L<sub>f</sub> = latent heat of freezing shrimp (kJ/Kg)

5. Efficiency of the refrigeration system (n)

$$n = \left( \frac{COP_{actual}}{COP_{carnot}} \right) \times 100$$

This efficiency is expressed as a percentage and calculated as the ratio between the actual coefficient of performance (COP)

Table 3 Physical properties of shrimp products

Shrimp character	Value*
C shrimp (specific heat of fresh shrimp)	3.75 kJ/kg°C
C shrimp (specific heat of frozen shrimp)	1.89 kJ/kg°C
Average temperature	5 °C
Shrimp freezing point	-1.94 °C
Freezing point of water	0 °C
Latent heat of shrimp	253.5 kJ/kg°C
C <sub>air</sub> = (specific heat of air)	4.18 kJ/kg°C

\*(Samsi *et al.*, 2023)

of the system and the Carnot COP, which represents the “theoretical” value derived from the condensation and evaporation temperatures (Srithar *et al.*, 2025). The percentages of COP<sub>Carnot</sub> efficiency levels are presented in Table 4.

**Shrimp Test Method**

Shrimp samples were evaluated during the first 20 h of storage in an air blast freezer (ABF). All parameters were analyzed in triplicate at each interval. The pH was measured using a calibrated pH meter on homogenized tissue prepared at a 1:9 ratio, and texture (firmness) was assessed using a simple penetrometer applied to standardized muscle sections. Drip loss was determined gravimetrically by calculating the difference in the sample weight before and after controlled storage. Melanosis was visually evaluated using a simplified scoring scale. The water holding capacity (WHC) was quantified using a centrifugation-based method to determine the percentage of retained moisture. Ice crystal size was observed in thin frozen sections using microscopy. Total volatile base nitrogen (TVB-N) was measured using the Conway diffusion method, followed by alkaline titration (Kim *et al.*, 2020).

**Data Analysis**

All thermodynamic performance and shrimp quality parameters were analyzed descriptively and statistically to evaluate the temporal changes during the transient air-blast freezing. The thermodynamic parameters included airflow velocity, air-side temperature differential ( $\Delta T$ ), evaporator frosting mass, cooling capacity (Q), and the actual coefficient of performance (COP). The shrimp quality parameters included ice crystal

size, water-holding capacity (WHC), drip loss, texture, pH, melanosis, and TVB-N. The data are presented in the Results and Discussion sections as tables and figures according to the characteristics of each variable. Descriptive analysis was used to summarize the direction, pattern, and magnitude of changes, whereas statistical analysis was applied, where appropriate, to assess differences among freezing intervals and examine associations among measured parameters, particularly those related to frosting accumulation, airflow reduction, cooling capacity changes, COP variation, and shrimp quality responses.

**RESULTS AND DISCUSSION**  
**Transient ABF Thermodynamic Behavior**

Transient ABF Thermodynamic Behavior testing was carried out with three treatments at each time, as presented in Table 5.

Table 5 demonstrates a clear transient degradation of the ABF thermodynamic performance during the first 5 h of operation, characterized by a progressive decline in airflow ( $4.38 \rightarrow 2.62 \text{ m s}^{-1}$ ),  $\Delta T_{\text{air}}$  ( $6.48 \rightarrow 3.83 \text{ }^\circ\text{C}$ ), cooling capacity Q ( $28.99 \rightarrow 20.98 \text{ kW}$ ), and COP ( $3.51 \rightarrow 2.33$ ), concomitant with exponential frosting accumulation on the evaporator coil ( $0.09 \rightarrow 1.50 \text{ kg}$ ). The monotonic reduction in airflow indicates increasing aerodynamic resistance across the coil, which suppresses convective heat transfer and lowers the effective temperature gradient, thereby directly reducing the evaporator heat absorption and system energy efficiency (Boeng & Stahelin *et al.*, 2025; de Sa Sarmiento *et al.*, 2025). This coupled behavior confirms that early stage frost growth acts as a dominant transient thermal resistance

Table 4 COP<sub>Carnot</sub> efficiency level percentage (Fianti, 2023)

Efficiency level	Types of efficiency
>100%	Very Efficient
76 – 100%	Efficient
51- 75%	Less Efficient
26 - 50%	Not efficient
1 - 25%	Very Inefficient



Table 5 Transient ABF performance parameters during early operation

Time (h)	Average of 3 measurements each time				
	Airflow (m/s)	$\Delta T_{\text{air}}$ (°C)	Frosting (kg, coil)	Q (kW)	COP (-)
0.0	4.38	6.48	0.09	28.99	3.51
0.5	4.31	5.60	0.14	27.85	3.40
1.0	4.25	5.16	0.20	27.01	3.21
1.5	3.80	4.60	0.25	26.7	3.15
2.0	3.40	4.49	0.32	25.53	2.94
2.5	3.19	4.32	0.57	24.43	2.78
3.0	3.09	4.19	0.84	23.95	2.71
3.5	2.91	4.05	1.12	22.8	2.56
4.0	2.64	3.86	1.36	21.06	2.37
4.5	2.63	3.85	1.45	21	2.34
5.0	2.62	3.83	1.50	20.98	2.33
5.5	2.62	3.82	1.49	20.97	2.33
6.0	2.62	3.82	1.49	29.97	2.33

layer, impairing both sensible and latent heat exchanges and accelerating COP deterioration (Jia *et al.*, 2021; Kumar *et al.*, 2024).

The nearly linear decline in Q and COP relative to the frosting mass suggests a strong thermodynamic sensitivity of the system performance to surface blockage during the pre-steady freezing phase. These trends are consistent with recent refrigeration system analyses reporting that frost layer thickening reduces air-side heat transfer coefficients and increases pressure drop, ultimately decreasing system capacity by 15–35% within short operating cycles (Hermes *et al.*, 2021; P. Zheng *et al.*, 2025; C. Ma *et al.*, 2025). Furthermore,

studies on air-blast and cold-room evaporators have confirmed that early transient frosting critically determines downstream product freezing kinetics owing to reduced convective intensity and altered thermal uniformity (C. Wang *et al.*, 2022; S. Liu, Zhang, Li, *et al.*, 2024). Therefore, the dataset robustly supports the interpretation that transient frosting accumulation is the primary mechanistic driver of early ABF performance decay, with direct implications for freezing rate stability and energy efficiency optimization in export-grade shrimp-processing systems (Cezar *et al.*, 2020; Yu *et al.*, 2021; Ye *et al.*, 2024).

Table 6 Pearson correlation matrix (r) calculation (n =11)

Variable	Airflow	$\Delta T$	Frosting	Q	COP
Airflow	1.000	0.992	-0.983	0.994	0.996
$\Delta T$	0.992	1.000	-0.975	0.989	0.991
Frosting	-0.983	-0.975	1.000	-0.987	-0.989
Q	0.994	0.989	-0.987	1.000	0.998
COP	0.996	0.991	-0.989	0.998	1.000

Table 7 Linear regression models of early-stage ABF performance

Dependent variable	Regression equation	R	R <sup>2</sup>	Adjusted R <sup>2</sup>	p-value	Interpretation
COP (-)	3.64 – 0.86 (Frosting)	0.989	0.978	0.975	<0.001	97.8% of COP variance explained by frost accumulation
Q (kW)	29.42 – 5.68 (Frosting)	0.987	0.973	0.970	<0.001	Cooling capacity strongly suppressed by frost growth
Airflow (m/s)	4.47 – 1.25 (Frosting)	0.983	0.966	0.962	<0.001	Frost formation directly restricts airflow

Pearson correlation analysis, justified by Shapiro-Wilk normality testing ( $p > 0.05$  for all variables), revealed an exceptionally strong thermodynamic coupling among the frosting mass, airflow,  $\Delta T$ , evaporator cooling capacity (Q), and COP during the first 5 h of ABF operation. Frosting exhibited a near-perfect negative association with COP ( $r = -0.989$ ,  $p < 0.001$ ) and airflow ( $r = -0.983$ ,  $p < 0.001$ ), whereas airflow was strongly correlated with Q ( $r = 0.994$ ) and COP ( $r = 0.996$ ), confirming a tightly synchronized degradation pathway (Alarcón-Gallén *et al.*, 2025; Jiao *et al.*, 2024). Linear regression further demonstrated that COP decline can be robustly predicted from frosting accumulation according to  $COP = 3.64 - 0.86(\text{Frosting})$  with  $R^2 = 0.978$ , indicating that nearly 98% of COP variance during early operation is explained by frost growth. Similarly,  $Q = 29.42 - 5.68(\text{Frosting})$  ( $R^2 = 0.973$ ), substantiating that airflow obstruction induced by frost formation directly suppresses cooling capacity before steady-state conditions are reached (Klingebiel *et al.*, 2025; Kumar *et al.*, 2024).

These findings move beyond descriptive transient reporting by quantitatively resolving the mechanistic cascade responsible for the early stage performance decay. The process begins with frost deposition on the evaporator surface, which progressively restricts the airflow within the freezing chamber. This airflow restriction reduces the effective heat transfer gradient between the cooling air and the product, leading to the suppression of the

cooling capacity of the system. The decline in cooling capacity subsequently results in a measurable degradation of the coefficient of performance (COP).

The results demonstrate that efficiency loss in industrial Air Blast Freezer (ABF) systems is not merely a time-dependent phenomenon but a statistically predictable process governed by the underlying mechanistic interactions occurring during the early stages of operation (Wang *et al.*, 2024; Wu *et al.*, 2024; Munk *et al.*, 2026). The near-deterministic correlations observed in this study highlight a critical and previously under-quantified early operation vulnerability window, offering a predictive framework that can be integrated with product quality kinetics to bridge machine performance dynamics and shrimp microstructural degradation (Food and Drug Administration, 2022; Xu *et al.*, 2024; Zhang *et al.*, 2025).

### Time-Resolved Shrimp Quality Changes

The changes in shrimp quality attributes during the first 6 h of ABF operation were evaluated to describe the early stage deterioration pattern associated with freezing performance (Table 8).

The time-resolved quality profile presented in Table 8 demonstrates a clear dynamic response of shrimp muscle properties during the first 6 h of ABF operation, characterized by an early rapid transition phase, followed by a progressive attenuation



Table 8 Mean Quality dynamics of frozen shrimp during first 6 h ABF operation

Time (h)	Meat pH	Texture (N)	Drip loss (%)	Melanosis (score)	WHC (%)	Ice crystal ( $\mu\text{m}$ )	TVB-N (mg N/100g)
0.0	6.95	11.0	1.80	0.9	86.0	8.0	14.0
0.5	6.97	10.8	1.90	1.0	85.0	9.0	14.5
1.0	6.99	10.4	2.00	1.1	83.0	10.0	15.0
2.0	7.04	9.9	2.20	1.2	81.0	11.0	16.0
3.0	7.07	9.4	2.30	1.3	79.0	13.0	17.0
4.0	7.10	9.0	2.40	1.4	78.0	14.0	18.0
5.0	7.11	8.8	2.50	1.5	77.0	15.0	18.0
6.0	7.11	8.7	2.52	1.5	76.8	15.2	18.2

of change. At the onset (0-1 h), quality parameters exhibited moderate but consistent shifts, with ice crystal size increasing from 8 to 10  $\mu\text{m}$  and WHC declining from 86% to 83%, accompanied by a slight rise in drip loss (1.80-2.00%) and a gradual reduction in texture firmness (11.0-10.4 N). This initial phase reflects the structural adjustment of muscle tissue during primary ice nucleation and crystal growth (Zhang *et al.*, 2021; Zhang *et al.*, 2020; Ahmad *et al.*, 2025). Between 2-4 h, the rate of deterioration became more pronounced: ice crystals enlarged from 11 to 14  $\mu\text{m}$ , WHC decreased further to 78%, and firmness dropped to 9.0 N, while drip loss increased to 2.40%. This period indicates intensified intracellular damage, likely associated with reduced freezing efficiency and increased thermal resistance within the system (Liu *et al.*, 2024).

Notably, the melanosis score rose progressively (0.9-1.4), suggesting that oxidative and enzymatic reactions continued despite subzero conditions (Han & Gokoglu, 2022; (Kittiphattanabawon *et al.*, 2024; Durage *et al.*, 2025). After 4 h, the system entered a quasi-stagnation phase, where changes became marginal; the ice crystal size increased only slightly (15.0-15.2  $\mu\text{m}$ ), WHC decline slowed (77-76.8%), and drip loss plateaued (2.50-2.52%). The stabilization of pH (7.11) and the minimal increment in TVB-N (18-18.2 mg

N/100 g) further indicate that early structural degradation predominates over biochemical spoilage within this time window (Sun *et al.*, 2023a; Alam *et al.*, 2023c). Overall, the data reveal a distinct critical period within the first 2-4 h, in which ABF performance exerts the strongest influence on microstructural integrity, while beyond 5 h, the deterioration trend approaches a steady-state condition (Ji *et al.*, 2021), highlighting the importance of controlling transient freezing efficiency during the early operational stage to preserve export-grade shrimp quality (Food and Drug Administration, 2022; Wei *et al.*, 2024; Xu *et al.*, 2025; Zheng *et al.*, 2026).

Table 9 demonstrates a robust and sequential thermodynamic-microstructural-functional linkage during the first 0-6 h of ABF operation, confirming that system performance deterioration propagates mechanistically toward product quality loss. The regression results indicate that COP exerts a strong and significant negative influence on ice crystal size ( $\beta = 4.94$ ;  $R^2 = 0.97$ ;  $p < 0.001$ ), indicating that declining refrigeration efficiency directly promotes larger ice crystal formation (Minh, 2023). In turn, ice crystal size significantly reduced water-holding capacity ( $\beta = -1.17$ ;  $R^2 = 0.96$ ;  $p < 0.001$ ), reflecting the structural disruption of muscle fibers and increased extracellular ice growth. Subsequently, WHC showed a

Table 9 Sequential linear regression model of thermodynamic-microstructural-functional quality relationship during 0-6 h ABF operation

Regression pathway	Regression equation	$\beta$ (slope)	R <sup>2</sup>	p-value	Interpretation
COP → Ice crystal size (μm)	Ice crystal = 25.62 - 4.94(COP)	-4.94	0.97	<0.001	Decreasing COP significantly enlarges ice crystals
Ice crystal size → WHC (%)	WHC = 94.52 - 1.17(Ice crystal)	-1.17	0.96	<0.001	Larger crystals significantly reduce water-holding capacity
WHC → drip loss (%)	Drip loss = 6.42 - 0.047(WHC)	-0.047	0.98	<0.001	Lower WHC strongly increases drip loss
Total indirect effect (COP → drip loss)	Drip loss ≈ f(COP) via mediators	—	0.94	<0.001	COP indirectly controls drip loss through structural damage

strong inverse relationship with drip loss ( $\beta = -0.047$ ;  $R^2 = 0.98$ ;  $p < 0.001$ ), confirming that reduced structural integrity translates into higher exudate release upon thawing (Sun *et al.*, 2023a, 2023b). The total indirect pathway (COP → Ice Crystal → WHC → Drip Loss) exhibited high explanatory power ( $R^2 = 0.94$ ;  $p < 0.001$ ), substantiating that COP does not merely represent an operational efficiency indicator but functions as a predictive upstream determinant of shrimp quality degradation through structural mediation (Klunklin *et al.*, 2025; X. Zheng *et al.*, 2026). Collectively, these findings provide quantitative evidence of a cascading cause-effect mechanism, positioning COP as an early thermodynamic control variable that governs microstructural stability and final functional quality during transient ABF performance.

### Coupled Machine-Product Interaction

The transient behavior of the ABF operation was analyzed in relation to ice crystal development to illustrate how changes in freezing performance influence the microstructural formation in shrimp products (Figure 1).

Figure 1 illustrates the inverse dynamic relationship between the actual coefficient of performance (COP) of the Air Blast Freezer

(ABF) and the evolution of ice crystal size during the first six hours of freezing. At the initial stage (0-1 h), the COP remains relatively high (3.5-3.2), corresponding to smaller ice crystal dimensions (8-10 μm), indicating efficient heat extraction and rapid surface freezing (Han & Gokoglu, 2022; Saini *et al.*, 2021). As the operation progressed, a gradual decline in COP was observed, reaching approximately 2.3 at 6 h. This thermodynamic deterioration coincided with a steady increase in the ice crystal size to 15 μm. The data suggest that transient efficiency loss, likely associated with frosting accumulation and reduced heat transfer capacity, directly influences freezing kinetics, allowing slower intracellular water solidification and promoting larger crystal formation (S. Liu, Zhang, Li, *et al.*, 2024; S *et al.*, 2023). This pattern confirms that early stage ABF stability plays a decisive role in controlling the microstructural integrity of shrimp muscle during freezing, establishing a mechanistic link between machine performance and product quality (Tan *et al.*, 2021; Yan *et al.*, 2023).

Figure 2 demonstrates a clear divergence between the water holding capacity (WHC) and drip loss throughout the first six hours of freezing. WHC showed a progressive decline from approximately 86% at the initial stage to below 77% at hour six, indicating a

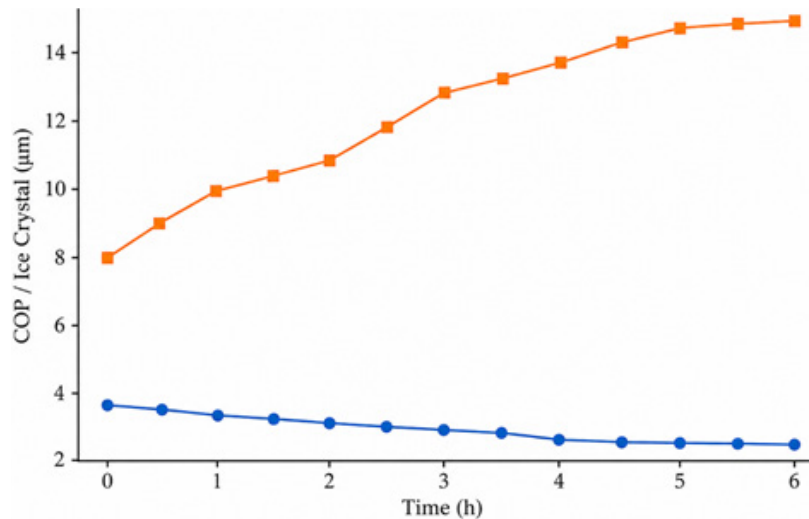


Figure 1 Transient ABF versus ice crystal development; (●) = COP; (■) ice crystal size

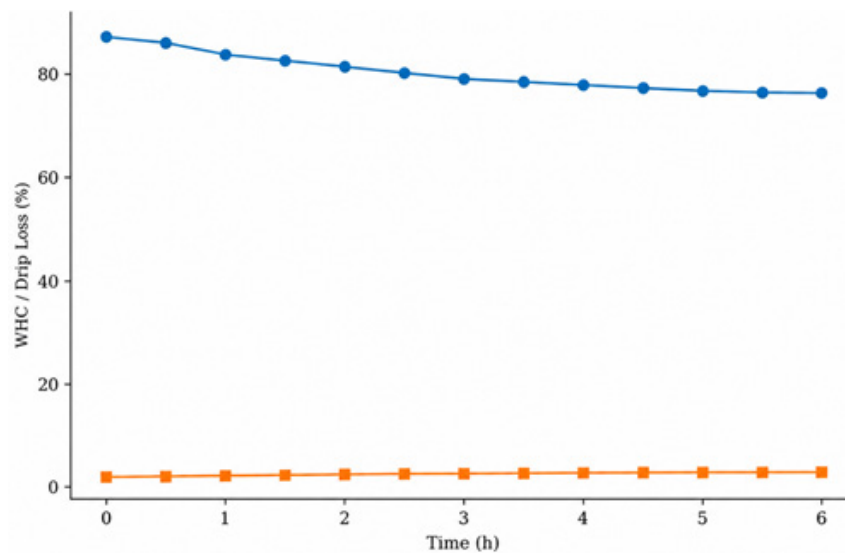


Figure 2 Time-resolved changes in WHC and drip loss; (●) = WHC (%), (■) = drip loss (%)

gradual impairment of the muscle's ability to retain intracellular water (Li *et al.*, 2024; Kamali *et al.*, 2024). In parallel, drip loss increased consistently from approximately 1.8% to approximately 2.5%, reflecting intensified exudate release during thawing (Q. Sun, Zhang, Yang, Hou, *et al.*, 2023; Yan *et al.*, 2023). The near-linear and opposing trajectories of these two parameters indicate a strong inverse association between structural water retention and the physical moisture loss. The transition becomes more pronounced after approximately three hours, suggesting that cumulative microstructural damage, likely associated with enlarging ice crystals,

compromises cellular integrity and accelerates extracellular fluid migration (Zhou *et al.*, 2026; Klunklin *et al.*, 2025). Collectively, the data confirm that transient freezing dynamics critically influence functional quality attributes, with a declining WHC serving as a precursor to measurable drip loss escalation.

Figure 3 presents the interaction between freezing time and system performance (COP) in terms of drip-loss development. During the high-COP phase (0-3 h), the drip loss increased gradually from approximately 1.8% to 2.3%, indicating controlled moisture migration under relatively stable thermodynamic conditions (Bao *et al.*, 2023).

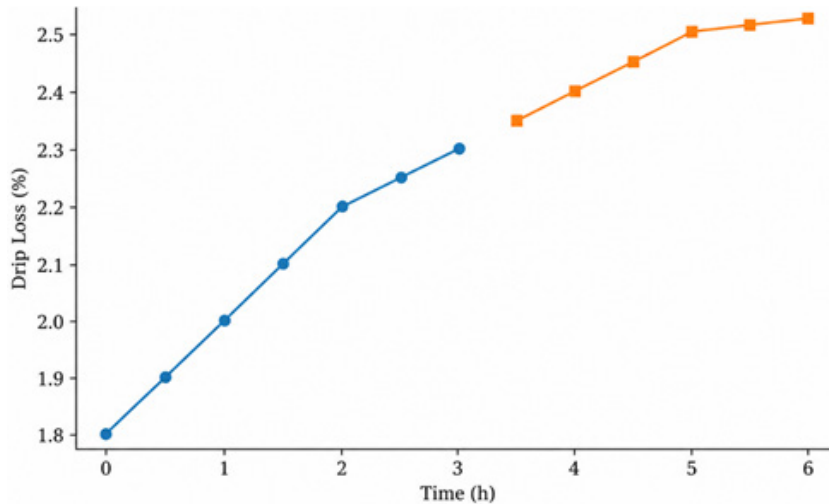


Figure 3 Interaction effect of time and COP on drip loss; (●) = the early observation period, (■) = the later observation period

In contrast, once the system transitioned into the lower COP phase ( $\geq 3.5$  h), the slope of the drip loss became steeper, rising to 2.5% by hour six. This divergence suggests that freezing time alone does not fully explain quality degradation; rather, the combined effects of prolonged exposure and reduced refrigeration efficiency amplify structural damage. This interaction pattern supports the hypothesis that early stage thermodynamic stability moderates moisture retention, whereas declining COP intensifies exudative losses (Skonieczny *et al.*, 2026; Y. Zhao *et al.*, 2025; K. Sun, Pan, Chen, Tao, *et al.*, 2023; L. Liu *et al.*, 2023; Phan *et al.*, 2021). Thus, the time  $\times$  COP interaction highlights a critical operational window in which maintaining a higher system efficiency can substantially

mitigate quality deterioration.

Figure 4 depicts the decomposition of the standardized effects linking COP to the drip loss through a mediation framework. The direct effect of COP on drip loss was negligible and slightly negative (-0.01), indicating that thermodynamic efficiency does not substantially influence moisture loss in the absence of structural intermediaries (Diao *et al.*, 2021; Wei *et al.*, 2024). In contrast, the indirect effect, quantified at approximately 0.265, dominated the relationship and closely approximated the total effect (0.255). This pattern confirms that the influence of COP on drip loss operates primarily through an intermediate variable, most plausibly ice crystal enlargement, and subsequent microstructural disruption (Z. Jin *et al.*, 2024;

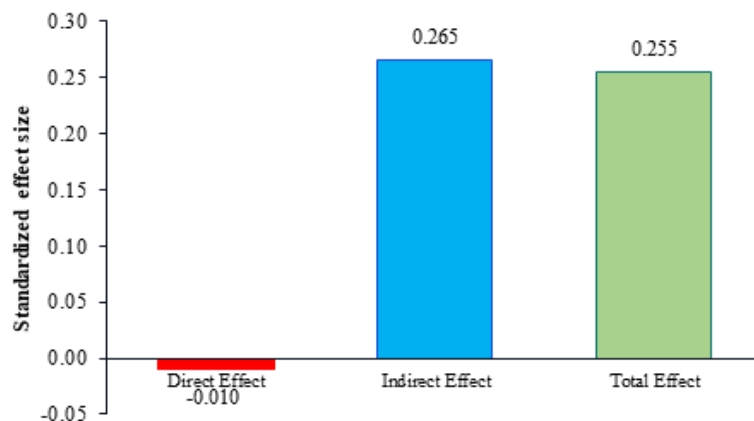


Figure 4 Mediation decomposition of COP effect on drip loss



O. Zheng *et al.*, 2024). The near equivalence between the indirect and total effects suggests a strong mediation pathway, reinforcing the mechanistic chain whereby declining refrigeration efficiency alters freezing kinetics, modifies crystal morphology, and ultimately increases exudative losses. Collectively, the mediation analysis substantiates that product quality deterioration is not directly driven by energy performance alone, but by its downstream impact on the structural integrity.

Figure 5 shows the critical transition point in the drip loss development during the first six hours of freezing. Drip loss increased moderately from approximately 1.8% at initiation to approximately 2.3% by the third hour, reflecting relatively controlled structural stress under stable freezing conditions (Giannakourou & Dermesonlouoglou, 2024; Guo *et al.*, 2022). However, beyond the ~3 h threshold, the trajectory approaches a steeper ascent toward  $\pm 2.5\%$ , indicating accelerated exudative release (LAO *et al.*, 2024; Wei *et al.*, 2025). Therefore, the vertical demarcation at hour three therefore represents a pivotal operational window, after which cumulative thermodynamic inefficiencies and microstructural damage become more pronounced (Yan *et al.*, 2023; Zhou *et al.*, 2026; Kim *et al.*, 2020). This inflection suggests that maintaining optimal system performance during the early freezing phase is essential to limit irreversible water migration.

Consequently, the data support the concept of a “critical freezing window” in which proactive control of heat transfer efficiency can significantly mitigate subsequent quality degradation.

The most decisive finding of this study is that early stage frost accumulation is the primary upstream driver of both thermodynamic degradation and shrimp microstructural deterioration during transient ABF operation. Frost growth during the first operational hours systematically reduced the airflow, suppressed the air-side temperature gradient, and diminished the cooling capacity and COP with near-deterministic statistical strength. These air-side reductions were synchronously associated with progressive ice crystal enlargement, declining water-holding capacity, and increasing drip loss, confirming that refrigeration efficiency functions as a quality-governing variable rather than merely an energy performance indicator (Wang Xu *et al.*, 2024; da Silva Oliveira & Gonçalves, 2019; Sánchez-Vega *et al.*, 2024).

Mechanistically, frost deposition increases the thermal resistance and pressure drop across the evaporator, thereby weakening the convective heat transfer intensity (P. Zheng *et al.*, 2025). Reduced convective extraction plausibly slows surface heat removal from shrimp tissue, extending the product’s residence time within the critical crystallization temperature zone (approximately  $-1$  to

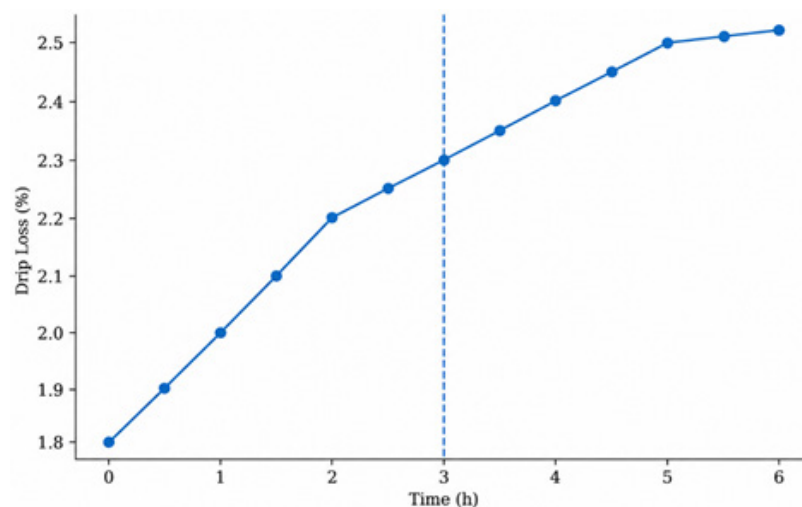


Figure 5 Identification of the critical freezing window; (●) = drip loss (%), (---) = the 3 h reference point

-5 °C), where crystal growth kinetics are highly sensitive to the freezing rate. It is important to distinguish direct evidence from thermodynamic inference: airflow, COP, and structural quality parameters were empirically measured, whereas prolonged residence time in the critical zone was inferred from air-side degradation and crystal enlargement patterns (Alarcón-Gallén *et al.*, 2025; Hermes *et al.*, 2021). Although the product core temperature was not instrumentally monitored, the exceptionally strong inverse regression between the COP and ice crystal size supports the plausibility of this mechanistic pathway.

When compared critically with existing refrigeration and frozen seafood studies, the magnitude of the cooling capacity and COP reduction observed in this study aligns with previously reported frost-induced performance losses in industrial evaporators. However, most earlier investigations have treated frosting as an isolated energy efficiency issue or have evaluated shrimp microstructure independently of system thermodynamics. This study advances beyond descriptive alignment by statistically integrating machine performance and product structural response into a sequential mediation framework (COP → Ice Crystal → WHC → Drip Loss), thereby resolving the mechanistic cascade with high explanatory power. This integrative perspective reveals a distinct early operational vulnerability window (approximately 2-4 h), during which thermodynamic instability exerts the strongest influence on crystal morphology before quasi-stable conditions emerge.

From an operational and HACCP standpoint, airflow decline exceeding approximately one-third of the baseline, COP approaching 3.0, or frost mass nearing 1.0-1.2 kg may serve as practical early warning indicators of accelerated structural degradation. Nevertheless, while the regression pathways exhibit strong predictive capability, the mechanistic interpretation remains confined to measured air-side and structural variables; direct validation of residence time dynamics requires embedded core temperature monitoring and high-

resolution freezing rate analysis in future investigations.

## CONCLUSION

This study demonstrates that early stage performance decay in air-blast freezer operation directly contributes to microstructural and functional quality deterioration in shrimp during the first 6 h of freezing. Frost accumulation reduced airflow, cooling capacity, and COP, whereas the decline in COP was strongly associated with ice crystal enlargement, reduced water-holding capacity, increased drip loss, and texture weakening. These findings position COP as a predictive upstream control parameter for connecting machine performance with product integrity, providing a practical basis for ABF optimization and HACCP-integrated quality monitoring in industrial shrimp-freezing systems.

## REFERENCES

- Ahmad, A. S., Sae-Leaw, T., Zhao, Y., Ma, L., Zhang, B., Hong, H., & Benjakul, S. (2025). Synergistic effects of selected nonthermal technologies combined with soursop leaf extract on the quality and shelf life of refrigerated *pacific white shrimp*. *Foods*, 14(8). <https://doi.org/10.3390/foods14081388>
- Alam, A., Solberg, C., & Hashem, M. (2023). Muscle histology and sensory quality changes during freeze storage of north atlantic shrimps (*Pandulus borealis*). *Meat Research*, 3(3), 1–4. <https://doi.org/10.55002/mr.3.3.60>
- Alar, E., Reindl, D., Nellis, G., & Young, T. (2024). Optimizing airflow in spiral blast freezers. *International Journal of Refrigeration*, 167, 177–184. <https://doi.org/https://doi.org/10.1016/j.ijrefrig.2024.07.015>
- Alarcón-Gallén, D., Marchante-Avellaneda, J., Hassan, A. H., & Navarro-Peris, E. (2025). Experimental study about frost formation and growth in the evaporator of an air-to-water heat pump. *International Journal of Refrigeration*, 179, 295–303. <https://doi.org/https://doi.org/https://doi.org/10.1016/j.ijrefrig.2025.01.015>



- doi.org/10.1016/j.ijrefrig.2025.08.013
- Anggrahini, D., Karningsih, P.D., & Sulistiyono, M. (2015). Managing quality risk in a frozen shrimp supply chain: a case study. *Procedia Manufacturing*, 4(Iess), 252–260. <https://doi.org/10.1016/j.promfg.2015.11.039>
- Badri, D., Toublanc, C., Rouaud, O., & Havet, M. (2021). Review on frosting, defrosting and frost management techniques in industrial food freezers. *Renewable and Sustainable Energy Reviews*, 151, 111545. <https://doi.org/https://doi.org/10.1016/j.rser.2021.111545>
- Bao, H., Zhang, J., Li, M., Chen, Y., Mao, C., Yang, J., Gao, Y., & Deng, S. (2023). Effect of freezing-thawing on the quality changes of large yellow croaker treated by low-salt soaking during frozen storage. *Frontiers in Nutrition*, 9, 1103838. <https://doi.org/10.3389/fnut.2022.1103838>
- Boeng, J., & Stahelin, R. (2025). Experimental investigation of frost accretion on microchannel evaporators for household refrigerators. *International Journal of Heat and Mass Transfer*, 250, 127327. <https://doi.org/https://doi.org/10.1016/j.ijheatmasstransfer.2025.127327>
- Cezar, C., Pimenta, N., & Seixlack, A. L. (2020). Influence of frost formation in tube-fin evaporators using a distributed model. *Proceedings of the XLI Ibero-Latin-American Congress on Computational Methods in Engineering*, ABMEC Foz do Iguaçu/PR, Brazil, November 16-19.
- Cheng, Y., Liu, X., Shi, J., Fu, S., Yang, H., Wu, L., Lou, Y., & Li, Y. (2025). Effect of thermostatic freezing on physicochemical indexes and metabolism of shrimp (*Solenocera melantho*). *Food Bioscience*, 68, 106403. <https://doi.org/https://doi.org/10.1016/j.fbio.2025.106403>
- da Silva Oliveira, M. É., & Gonçalves, A. A. (2019). The effect of different food grade additives on the quality of pacific white shrimp (*Litopenaeus vannamei*) after two freeze-thaw cycles. *LWT*, 113, 108301. <https://doi.org/https://doi.org/10.1016/j.lwt.2019.108301>
- de Sa Sarmiento, F., Sarmiento, A. P., & Ohadi, M. (2025). Control of frost formation in refrigeration applications utilizing the electrohydrodynamic technique—fundamentals, past work and prospects. *Philosophical Transactions of the Royal Society A: Mathematical, Physical and Engineering Sciences*, 383(2301), 20240364. <https://doi.org/10.1098/rsta.2024.0364>
- Diao, Y., Cheng, X., Wang, L., & Xia, W. (2021). Effects of immersion freezing methods on water holding capacity, ice crystals and water migration in grass carp during frozen storage. *International Journal of Refrigeration*, 131, 581–591. <https://doi.org/https://doi.org/10.1016/j.ijrefrig.2021.07.037>
- Duan, K., Sun, L., Geng, J., Yang, W., Wei, H., Huang, T., & Jia, R. (2025). Protein structural transitions and cryo-stability of shrimp gel: Effects of setting time at 30°C in a novel processing system. *Innovative Food Science & Emerging Technologies*, 105, 104191. <https://doi.org/https://doi.org/10.1016/j.ifset.2025.104191>
- Durage, T. T. D. (2025). Replacing Sodium Tripolyphosphate in Frozen Shrimp Preservation: Soaking Treatments, Nonthermal Technologies, and Their Limitations. *Journal of Food Science*, 90(7), e70365. <https://doi.org/10.1111/1750-3841.70365>
- [FDA] Food and Drug Administration. (2022). Fish and fishery products hazards and controls guidance. *Fish and Fishery Products Hazard and Control Guidance Fourth Edition, June*, 1–401.
- Fianti. (2023). Coefficient of Performance pada coldstorage PT IMPD/PT WIFI Sorong. *Jurnal Voering*, 8(1), 29–34. <https://doi.org/10.32531/jvoe.v8i1.814>
- Giannakourou, M. C., & Dermesonlouoglou, E. (2024). 12 - Quality kinetics and shelf life prediction and management in the frozen foods chain. In S. M. Jafari & H. Rostamabadi (Eds.), *Low-Temperature Processing of Food Products* (pp. 289–327). Woodhead Publishing. <https://doi.org/https://doi.org/10.1016/B978-0-12-818733-3.00008-4>

- Guo, F., Qian, K., Li, X., & Deng, H. (2022). Simulation study of cell transmembrane potential and electroporation induced by time-varying magnetic fields. *Innovative Food Science & Emerging Technologies*, 81, 103117. <https://doi.org/https://doi.org/10.1016/j.ifset.2022.103117>
- Han, A., & Gokoglu, N. (2022). Effects of different freezing and thawing methods on the quality of giant red shrimp (*Aristaeomorpha foliacea*). *Acta Aquatica: Aquatic Sciences Journal*, 9, 46. <https://doi.org/10.29103/aa.v9i1.6410>
- Hermes, C. J. L., Boeng, J., da Silva, D. L., Knabben, F. T., & Sommers, A. D. (2021). Evaporator frosting in refrigerating appliances: Fundamentals and Applications. *Energies*, 14(18). <https://doi.org/10.3390/en14185991>
- Ji, W., Bao, Y., Wang, K., Yin, L., & Zhou, P. (2021). Protein changes in shrimp (*Metapenaeus ensis*) frozen stored at different temperatures and the relation to water-holding capacity. *International Journal of Food Science and Technology*, 56(8), 3924–3937. <https://doi.org/10.1111/ijfs.15009>
- Jia, L., Shen, J., Hu, K., & Zhu, T. (2021). Experimental study on the effect of heat transfer temperature difference on frosting characteristics of air-cooled heat exchanger. *IOP Conference Series: Earth and Environmental Science*, 791, 12123. <https://doi.org/10.1088/1755-1315/791/1/012123>
- Jiao, F., Li, G., Zhang, C., & Liu, J. (2024). Study on the coupling of air-source heat pumps (ASHPs) and Passive Heating in cold regions. *Buildings*, 14(8). <https://doi.org/10.3390/buildings14082410>
- Jin, L., Ding, G., Li, P., Gu, J., & Zhang, X. (2018). Changes in quality attributes of marine-trawling shrimp (*Solenocera crassicornis*) during storage under different deep-frozen temperatures. *Journal of Food Science and Technology*, 55(8), 2890–2898. <https://doi.org/10.1007/s13197-018-3207-x>
- Jin, Z., Jiang, C., Sun, B., Liu, J., & Sun, W. (2024). Incomplete freezing strategies for achieving long-lasting preservation of muscle foods: categories, regulations, efficiencies and challenges. *Food Science of Animal Products*, 2(3), 9240075. <https://doi.org/10.26599/FSAP.2024.9240075>
- Kamali, M., Shabanpour, B., Pourashouri, P., & Kordjazi, M. (2024). Evaluating shelf life and anti-browning of shrimp by chitosan-coated nanoliposome loaded with licorice root extract. *Food Chemistry: X*, 23, 101532. <https://doi.org/10.1016/j.fochx.2024.101532>
- Kim, S.-H., Jung, E.-J., Hong, D.-L., Lee, S.-E., Lee, Y.-B., Cho, S., & Kim, S.-B. (2020). Quality assessment and acceptability of whiteleg shrimp (*Litopenaeus vannamei*) using biochemical parameters. *Fisheries and Aquatic Sciences*, 23(1), 21. <https://doi.org/10.1186/s41240-020-00167-6>
- Kittiphattanabawon, P., Temdee, W., Maqsood, S., Visessanguan, W., & Benjakul, S. (2024). Gelatin hydrolysate in freeze-thawed shrimp model system: retardation of weight loss and muscle protein denaturation. *International Journal of Food Science and Technology*, 59(7), 4949–4957. <https://doi.org/10.1111/ijfs.17227>
- Klingebliel, J., Höges, C., Horst, J., Nießen, O., Venzik, V., Vering, C., & Mueller, D. (2025). A self-optimizing defrost initiation controller for air-source heat pumps: Experimental validation of deep reinforcement learning. *Applied Energy*, 398, 126400. <https://doi.org/10.1016/j.apenergy.2025.126400>
- Klunklin, W., Fong-in, S., & Klinmalai, P. (2025). Investigating the microstructural and cryoprotective superiority of fructooligosaccharides and sugar alcohols for maintaining peeled white shrimp (*Litopenaeus vannamei*) quality after repeated freeze-thaw cycles. *LWT*, 233, 118526. <https://doi.org/https://doi.org/10.1016/j.lwt.2025.118526>
- Kumar, M., Kiran, K. K., Mondal, S., Khan, M. A., Khan, T. M. Y., Almakayeel, N., & Khan, W. A. (2024). Performance evaluation of evaporator coil of a domestic refrigerator under frosting.



- International Journal of Low-Carbon Technologies*, 19, 2746–2754. <https://doi.org/10.1093/ijlct/ctae232>
- Lao, M., Zeng, L., Wu, M., Wang, H., Peng, L., Wang, Q., Lu, H., Cao, N., & Jiao, C. (2024). Effects of freezing methods on water-holding capacity and structural properties of myofibrillar proteins from hind leg muscle of rana nigromaculata. *Food Science*, 45(13), 264–274. <https://doi.org/10.7506/spkx1002-6630-20231025-218>
- Li, Y., Han, X., Zhang, Y., Wang, Y., Wang, J., Teng, W., Wang, W., & Cao, J. (2024). Thawed drip and its membrane-separated components: Role in retarding myofibrillar protein gel deterioration during freezing-thawing cycles. *Food Research International*, 188, 114461. <https://doi.org/https://doi.org/10.1016/j.foodres.2024.114461>
- Lin, D., Sun, L.-C., Chen, Y.-L., Liu, G.-M., Miao, S., & Cao, M.-J. (2022). Shrimp spoilage mechanisms and functional films/coatings used to maintain and monitor its quality during storage. *Trends in Food Science & Technology*, 129, 25–37. <https://doi.org/https://doi.org/10.1016/j.tifs.2022.08.020>
- Liu, L., Jiao, W., Xu, H., Zheng, J., Zhang, Y., Nan, H., & Huang, W. (2023). Effect of rapid freezing technology on quality changes of freshwater fish during frozen storage. *LWT*, 189, 115520. <https://doi.org/https://doi.org/10.1016/j.lwt.2023.115520>
- Liu, S., Zhang, L., Chen, J., Li, Z., Liu, M., Hong, P., Zhong, S., & Li, H. (2024). Effect of freeze–thaw cycles on the freshness of prepackaged *Penaeus vannamei*. *Foods*, 13(2). <https://doi.org/10.3390/foods13020305>
- Liu, S., Zhang, L., Li, Z., Liu, M., Chen, J., Hong, P., Zhong, S., & Huang, J. (2024). Effect of temperature fluctuation on the freshness, water migration and quality of cold-storage *Penaeus vannamei*. *LWT*, 193, 115771. <https://doi.org/https://doi.org/10.1016/j.lwt.2024.115771>
- Ma, C., Ge, X., Zheng, H., Song, M., Sheng, W., Chen, X., Fu, D., & Dang, C. (2025). From common low temperature to ultra-low temperature: overview of frosting characteristics and defrosting techniques in equipment. *Applied Thermal Engineering*, 278, 127205. <https://doi.org/https://doi.org/10.1016/j.applthermaleng.2025.127205>
- Ma, J., & Thorade, M. (2024). Frost/Defrost Models for Air-Source Heat Pumps with Retained Water Refreezing Considered. Proceedings of the 16th International Modelica&FMI Conference, September 8 – 10, 2025, *Lucerne University of Applied Sciences and Arts (HSLU)*. <https://doi.org/10.48550/arXiv.2412.00017>
- Minh, N. P. (2023). Partial replacement of sodium pyrophosphate by xylitol and mannitol in white-leg shrimp (*Litopenaeus vannamei*) on its quality during frozen storage preservation. *Food Research*, 7(1), 113–119. [https://doi.org/10.26656/fr.2017.7\(1\).948](https://doi.org/10.26656/fr.2017.7(1).948)
- Munk, J., Marsik, T., Truffer-Moudra, D., Stevens, V., Dennehy, C., Winkler, J., & Strunk, R. (2026). Cold climate field study of the effect of defrost controls on the integrated performance of a ductless air-source heat pump. *Energies*, 19(3). <https://doi.org/10.3390/en19030733>
- Phan, D. T. A., Bui, T. H., Doan, T. Q. T., Nguyen, N. Van, & Ly, T. H. (2021). Inhibition of melanosis in whiteleg shrimp (*Litopenaeus vannamei*) during refrigerated storage using extracts of different avocado (*Persea americana Mill.*) by-products. *Preventive Nutrition and Food Science*, 26(2), 209–218. <https://doi.org/10.3746/pnf.2021.26.2.209>
- Prambudia, Y., & Sriwana, I. K. (2025). Dynamic system analysis of vannamei shrimp supply chain: evaluation of distribution delays in cold chain logistics at exporting companies. *Al-Kharaj: Journal of Islamic Economic and Business*, 7(2), 412–426. <https://ejournal.iainpalopo.ac.id/index.php/alkharaj/article/view/7694>
- S, V., Singha, P., Dasgupta, M. S., Hafner, A., Widell, K., Bhattacharyya, S., Saini, S. K., Arun, B. S., Samuel, M. P., & Ninan, G. (2023). Performance analysis of a

- CO<sub>2</sub>/NH<sub>3</sub> cascade refrigeration system with subcooling for low temperature freezing applications. *International Journal of Refrigeration*, 153, 140–154. <https://doi.org/https://doi.org/10.1016/j.ijrefrig.2023.05.013>
- Saini, S. K., Dasgupta, M. S., Widell, K. N., & Bhattacharyya, S. (2021). Comparative analysis of a few novel multi-evaporator CO<sub>2</sub>-NH<sub>3</sub> cascade refrigeration system for seafood processing & storage. *International Journal of Refrigeration*, 131, 817–825. <https://doi.org/https://doi.org/10.1016/j.ijrefrig.2021.07.017>
- Samanta, P., & Imroatin, K. (2025). Cold chain and shrimp product quality: impacts on market trust and production management. *Education and Social Sciences Review*, 6, 59–71. <https://doi.org/10.29210/07essr577700>
- Samsi, Hermawan, A., Binardi, T., Dewi, P., Ilham, M., & Rahardja, I. B. (2023). Analisa beban pendingin produk pada *contact plate freezer* terhadap kinerja kompresor di PT. Trimitra Makmur, Tarakan, Kalimantan Utara. *Teknologi*, 5(1), 68–78. <https://doi.org/10.24853/jurtek.15.2.207-216>
- Sánchez-Vega, R., Aguiló-Aguayo, I., & Rodríguez-Roque, M. J. (2024). 8 - Direct or indirect immersion freezing systems. In S. M. Jafari & H. Rostamabadi (Eds.), *Low-Temperature Processing of Food Products* (pp. 167–196). Woodhead Publishing. <https://doi.org/https://doi.org/10.1016/B978-0-12-818733-3.00007-2>
- Skonieczny, M., Królikowska, M., Padaszyński, K., & Więckowski, M. (2026). Thermodynamic properties and coefficient of performance calculations of {Choline thiocyanate, dicyanamide, tricyanomethanide + ethanol} systems for absorption refrigeration technology applications. *Fluid Phase Equilibria*, 600, 114548. <https://doi.org/https://doi.org/10.1016/j.fluid.2025.114548>
- Srithar, K., Venkatesan, R., Ram Bala Ganesh, S., & Leo Arockiasamy, S. (2025). The Implementation of humidification-dehumidification desalination system for COP enhancement in cold storage unit. *Cleaner Engineering and Technology*, 29, 101079. <https://doi.org/https://doi.org/10.1016/j.clet.2025.101079>
- Sun, K., Pan, C., Chen, S., Liu, S., Hao, S., Huang, H., Wang, D., & Xiang, H. (2023a). Quality changes and indicator proteins of *Litopenaeus vannamei* based on label-free proteomics analysis during partial freezing storage. *Current Research in Food Science*, 6, 100415. <https://doi.org/https://doi.org/10.1016/j.crfs.2022.100415>
- Sun, K., Pan, C., Chen, S., Tao, F., Liu, S., Zhao, Y., Li, C., & Wang, D. (2023b). Quality deterioration of *Litopenaeus vannamei* associated with protein changes during partial freezing storage. *Food Science of Animal Products*, 1(1), 9240002. <https://doi.org/10.26599/FSAP.2023.9240002>
- Sun, K., Pan, C., Chen, S., Wu, H., Liu, S., Hao, S., Huang, H., & Xiang, H. (2023c). Effect of water change on quality deterioration of pacific white shrimp (*Litopenaeus vannamei*) during partial freezing storage. *Food Chemistry*, 416, 135836. <https://doi.org/https://doi.org/10.1016/j.foodchem.2023.135836>
- Sun, Q., Zhang, H., Yang, X., Hou, Q., Zhang, Y., Su, J., Liu, X., Wei, Q., Dong, X., Ji, H., & Liu, S. (2023dsun). Insight into muscle quality of white shrimp (*Litopenaeus vannamei*) frozen with static magnetic-assisted freezing at different intensities. *Food Chemistry: X*, 17, 100518. <https://doi.org/https://doi.org/10.1016/j.fochx.2022.100518>
- Tan, M., Mei, J., & Xie, J. (2021). The Formation and control of ice crystal and its impact on the quality of frozen aquatic products: a review. *Crystals*, 11(1). <https://doi.org/10.3390/cryst11010068>
- Wang, C., You, Z., Ding, Y., Zhang, X., & She, X. (2022). Liquid air energy storage with effective recovery, storage and utilization of cold energy from liquid air evaporation. *Energy Conversion and Management*, 267, 115708. <https://doi.org/https://doi.org/10.1016/j.enconman.2022.115708>
- Wang, Z., Zhang, P., Wang, F., Ma, L., &



- Ma, Z. (2024). The study of dynamic characteristics on a novel air source heat pump coupled with liquid-storage gas-liquid separator under non frosting and refrigeration conditions. *Journal of Building Engineering*, 84, 108538. <https://doi.org/https://doi.org/10.1016/j.jobe.2024.108538>
- Wei, Q., Sun, Q., Dong, X., Kong, B., Ji, H., & Liu, S. (2024). Effect of static magnetic field-assisted freezing at different temperatures on muscle quality of pacific white shrimp (*Litopenaeus vannamei*). *Food Chemistry*, 438, 138041. <https://doi.org/https://doi.org/10.1016/j.foodchem.2023.138041>
- Wei, Q., Sun, Q., Hou, Q., Zheng, O., Xiao, N., & Liu, S. (2025). Effect of static magnetic field-assisted freezing at different temperatures on the structural and functional properties of pacific white shrimp (*Litopenaeus vannamei*) myofibrillar protein. *Food Chemistry*, 471, 142836. <https://doi.org/https://doi.org/10.1016/j.foodchem.2025.142836>
- Wu, S., Sun, Y., Wang, F., Ma, Z., Zhao, R., & Huang, D. (2024). A prediction model of air-source heat pump system performance with frost-retarded heater. *Applied Thermal Engineering*, 248, 123315. <https://doi.org/https://doi.org/10.1016/j.applthermaleng.2024.123315>
- Xu, W., Bao, Y., Gou, H., Xu, B., Hong, H., & Gao, R. (2024). Mitigation of mechanical damage and protein deterioration in giant river prawn (*Macrobrachium rosenbergii*) by multi-frequency ultrasound-assisted immersion freezing. *Food Chemistry*, 458, 140324. <https://doi.org/https://doi.org/10.1016/j.foodchem.2024.140324>
- Xu, Y., Zhao, R., Wu, K., Jin, H., Song, M., & Shen, X. (2024). Experimental investigation and validation on an air-source heat pump frosting state recognition method based on fan current fluctuation signal and machine learning. *Energy*, 291, 130372. <https://doi.org/https://doi.org/10.1016/j.energy.2024.130372>
- Xu, Z., Redo, M. A., Llave, Y., Koga, Y., & Watanabe, M. (2025). Effect of fan speed, sample orientation, and tray structure on heat transfer and food freezing time in batch air blast freezer. *International Journal of Thermal Sciences*, 214, 109915. <https://doi.org/https://doi.org/10.1016/j.ijthermalsci.2025.109915>
- Yan, W., Sun, Q., Zheng, O., Han, Z., Wang, Z., Wei, S., Ji, H., & Liu, S. (2023). Effect of liquid nitrogen freezing temperature on the muscle quality of *litopenaeus vannamei*. *Foods*, 12(24). <https://doi.org/10.3390/foods12244459>
- Ye, Z., Wang, W., Li, X., & Chen, J. (2024). Review on anti-frost technology based on microchannel heat exchanger. *Journal of Shanghai Jiaotong University (Science)*, 29(2), 161–178. <https://doi.org/10.1007/s12204-022-2539-x>
- Yu, B., Luo, Y., & Chu, W. (2021). Analysis on frosting of heat exchanger and numerical simulation of heat transfer characteristics using BP neural network learning algorithm. *PloS One*, 16(9), e0256836. <https://doi.org/10.1371/journal.pone.0256836>
- Zhang, B., Cao, H., Wei, W., & Ying, X. (2020). Influence of temperature fluctuations on growth and recrystallization of ice crystals in frozen peeled shrimp (*Litopenaeus vannamei*) pre-soaked with carrageenan oligosaccharide and xylooligosaccharide. *Food Chemistry*, 306, 125641. <https://doi.org/https://doi.org/10.1016/j.foodchem.2019.125641>
- Zhang, Y., He, F., Wang, Y., Li, C., Zhang, G., & Zhou, D. (2025). Recent advances, challenges and future prospects on frost-free air source heat pump technology with integrated solid desiccant dehumidification. *Renewable and Sustainable Energy Reviews*, 219, 115877. <https://doi.org/https://doi.org/10.1016/j.rser.2025.115877>
- Zhang, Y., Li, F., Yao, Y., He, J., Tang, J., & Jiao, Y. (2021). Effects of freeze-thaw cycles of Pacific white shrimp (*Litopenaeus vannamei*) subjected to radio frequency tempering on melanosis and quality. *Innovative Food Science & Emerging Technologies*, 74, 102860. <https://doi.org/https://doi.org/10.1016/j.ifs.2021.102860>

- ifset.2021.102860
- Zhao, X., Wang, L., Wang, J., Xu, Y., Zhu, W., Li, J., Cui, F., & Li, X. (2024). Effects of different freezing methods on muscle qualities and myofibrillar protein properties of red drum (*Sciaenops ocellatus*) during storage. *International Journal of Refrigeration*, 165, 199–208. <https://doi.org/https://doi.org/10.1016/j.ijrefrig.2024.05.021>
- Zhao, Y., Yang, Z., Hou, Z., & Zhang, S. (2025). Thermodynamic behavior and critical miscibility dynamics of refrigerant–lubricant mixtures for refrigeration and heat pump systems. *Journal of Molecular Liquids*, 438, 128730. <https://doi.org/https://doi.org/10.1016/j.molliq.2025.128730>
- Zheng, O., Hou, Q., Wei, Q., Sun, P., Cheng, W., Ding, L., Sun, Q., & Liu, S. (2024). Insights into the potential mechanism of diversified freezing techniques' influence on quality of golden pompano (*Trachinotus ovatus*): Focus on freezing speed, ice crystal morphology, water migration, and texture properties. *LWT*, 205, 116539. <https://doi.org/https://doi.org/10.1016/j.lwt.2024.116539>
- Zheng, P., Wang, T., Suo, W., Ohki, T., Iwamoto, T., Tanaka, M., Shi, S., Liu, S., Yang, P., & Liu, Y. (2025). Experimental study on the frosting characteristics and heat transfer performance of the flying-wing heat exchanger. *Results in Engineering*, 28, 108220. <https://doi.org/https://doi.org/10.1016/j.rineng.2025.108220>
- Zheng, X., Shi, H., Li, R., Chen, L., Li, Z., & Xue, C. (2026). Changes in the quality of aquatic products during liquid nitrogen quick-freezing: a review. *Agricultural Products Processing and Storage*, 2(1). <https://doi.org/10.1007/s44462-025-00047-z>
- Zhou, P., Zhang, X., Yu, H., Xu, L., Xu, D., Chen, X., & Wang, S. (2026). Effects of shipboard ultra-low-temperature freezing and plate freezing on quality of marine-caught shrimp based on numerical simulation and experimental evaluation. *LWT*, 241, 119109. <https://doi.org/https://doi.org/10.1016/j.lwt.2026.119109>
- Zhu, Z., Zhang, H., Liu, X., Zeng, Q., Sun, D.-W., & Wang, Z. (2024). In situ investigation of ice fractions and water states during partial freezing of pork loins and shrimps. *Food Chemistry*, 457, 140089. <https://doi.org/https://doi.org/10.1016/j.foodchem.2024.140089>